Elongational Viscosity of Polymer Melts: A Lubricated Skin-Core Flow Approach

AJIT V. PENDSE and JOHN R. COLLIER*

Department of Chemical Engineering, Louisiana State University, Baton Rouge, Louisiana 70803

SYNOPSIS

Previous work by this research group has shown that the use of a lubricated skin/core flow of polymer melts and a hyperbolic converging die results in an essentially pure elongational flow at a constant elongational strain rate in the core. The previous work was carried out on a laboratory-scale coextrusion system in a planar slit die; tracer particles and an image analysis system were used to confirm the predicted behavior. In this work, the technique was implemented first on the coextruder assembly, as a planar elongational rheometer, and then on a commercial capillary rheometer, as a uniaxial elongational rheometer for polymer melts. The later is achieved by replacing the standard capillary die with a hyperbolic axisymmetric die. A two-layered billet is prepared for placement in the rheometer barrel by completely encapsulating the core polymer (the polymer to be analyzed) with a low-viscosity polyethylene skin. Commercial grades of polypropylenes, syndiotactic polystyrene, and nylon-66 were analyzed using this technique. Elongational viscosity at high extensional rates can be determined with this method; values in excess of 500 s^{-1} have already been achieved. © 1996 John Wiley & Sons, Inc.

BACKGROUND

Shear rheometry is very well developed and there are several commercial rheometers available.[1,2] In the recent rheological literature, the importance of elongational rheometry has become apparent,[3] and the field is still growing. The motivation for the study of elongational flows is twofold: the realization that in several key industrial processes such as spinning, blow molding, injection molding, extrusion in converging dies, etc., the dominant mode of flow is elongational, and that shear rheology alone is not sufficient to characterize materials such as polymer melts and solutions.[4] Furthermore, elongational rheology, as a method of the characterization of materials, is not limited to polymer melts. It has recently attracted the attention of researchers from diverse areas such as rodlike micelles[5] and food processing of doughs.[6]

There are broadly four approaches used in elongational viscosity measurement: (1) indirect measurements, where the data from shear rheology is interpreted to obtain elongational parameters,[7] (2) use of unconfined flow in stretching devices,[8] (3) spinning,[9] and (4) lubricated flow.[10-12] Other techniques such as the opposed jet impingement technique[13] and the bubble collapse technique[14] have also been used to generate elongational flow fields. A detailed review of the available literature on elongational rheometry can be found elsewhere.[14-16]

The difficulty of generating steady and controlled elongational flow fields has severely restricted the development of commercial extensional rheometers; this is particularly evident in the range of extensional rates higher than 10 s^{-1}. This article describes an extensional rheometer that can be used to generate high extensional rates (up to 533 s^{-1}) that are closer to those typically observed in industrial operations.

In a previous article by this research group,[17] a technique was presented in which it was shown that an essentially pure elongational flow could be obtained in the core in skin–core coextrusion if the core-to-skin viscosity ratio of between 30 and 100 and the core to skin flow rate ratio of about 10 were maintained. Both the variables can be independently

* To whom correspondence should be addressed.

Journal of Applied Polymer Science, Vol. 59, 1305–1314 (1996)
 CCC 0021-8995/96/081305-10

controlled as they are externally applied. Since the stress at the interface is the same for the skin and the core, the high viscosity ratio (core-to-skin) causes the strain rate of the skin at the interface to be of the order of 100 times larger than the core at the interface, thereby causing the shearing gradient to essentially reside in the skin. By changing the flow rate ratio, the position of the interface is changed; therefore, the shear stress at the interface and the average shear strain rate in the skin layer are changed. The skin layer acts as a lubricating layer and the resultant shear stress and the pressure drop for a given flow rate for the coextrusion system is lowered.[18] It was shown by tracer-particle-measured velocity profiles that a steady and constant elongational flow field can be generated by using a hyperbolic converging slit die. In the present work, the technique is implemented on a commercial capillary rheometer. There are several advantages in doing so. First, the tried and tested material packing and data acquisition system of a commercial unit can be used; second, high flow rates that are available in shear measurement can be used to achieve high strain rates for elongational rheology; and, finally, after slight modifications, an elongational rheology technique can be available as an auxiliary unit to an existing commercial capillary rheometer.

METHODOLOGY

The planar elongational viscosity was determined in a coextrusion assembly. Two extruders, each fitted with a gear pump, were used to generate a skin–core flow in the hyperbolic die. Complete details of the assembly were described in a previous article.[17] A hyperbolic slit die of the following profile was used in the experiments:

$$y = \frac{B}{x + A}, \tag{1}$$

where A and B are geometry-defined constants.

The determination of uniaxial elongational viscosity was done by adapting the computer-controlled capillary rheometer ACER manufactured by Polymer Laboratories Ltd., U.K. (now a part of Rheometrics Inc., U.S.A.). A schematic of the ACER is shown in Figure 1. For shear rheometry, the polymer is packed in the cylindrical barrel, and a standard capillary die is fitted at the end of it. A drive section at the top moved the ram through the length of the barrel, pushing the polymer melt through the die at the programmed volumetric flow rate. A pressure

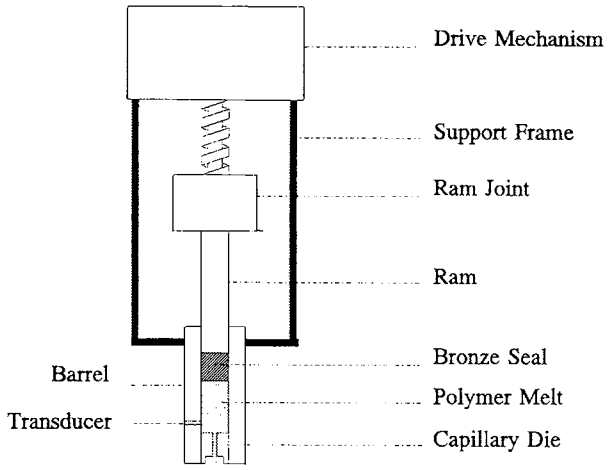

Figure 1 Schematic of the advanced capillary extrusion rheometer (ACER).

transducer attached flush with the wall of the barrel 5 mm above the die was used to measure the pressure drop across the die.

For elongational rheometry, the standard capillary die was replaced by a uniaxially converging hyperbolic die. Figure 2 shows the hyperbolic die designed for the experiment. The die was manufactured by Scientific Fabrication Service Inc., Plaquemine, LA. Electro-discharge machining was used to shape the inner die profile to the required design equation. The material used was Type D-2 Tool-steel. Corresponding to the available ram speed range, elongational strain rates of 2.665×10^{-1} -7.5×10^{2} s^{-1} can be achieved on this unit. The profile of the die was designed according to the following equation:

$$r^2 = \frac{C}{z + D}, \tag{2}$$

where C and D are geometry-defined constants.

The barrel was preheated to the required temperature and packed with the sample. In the case of shear rheology, the sample was charged in the barrel directly. Two-layer billets, with the polymer to be analyzed in the core completely encapsulated by the skin (polyethylene for all the experiments in this work), were prepared for elongational rheology experiments. A heat soak for 20 min was allowed for the samples to reach a thermal steady state prior to the start of the experiments. The range of shear (or elongational) strain rates were applied in steps of ram speeds, each speed corresponding to a fixed strain rate. The pressure drop across the die and the temperature of the melt were then recorded. Statis-

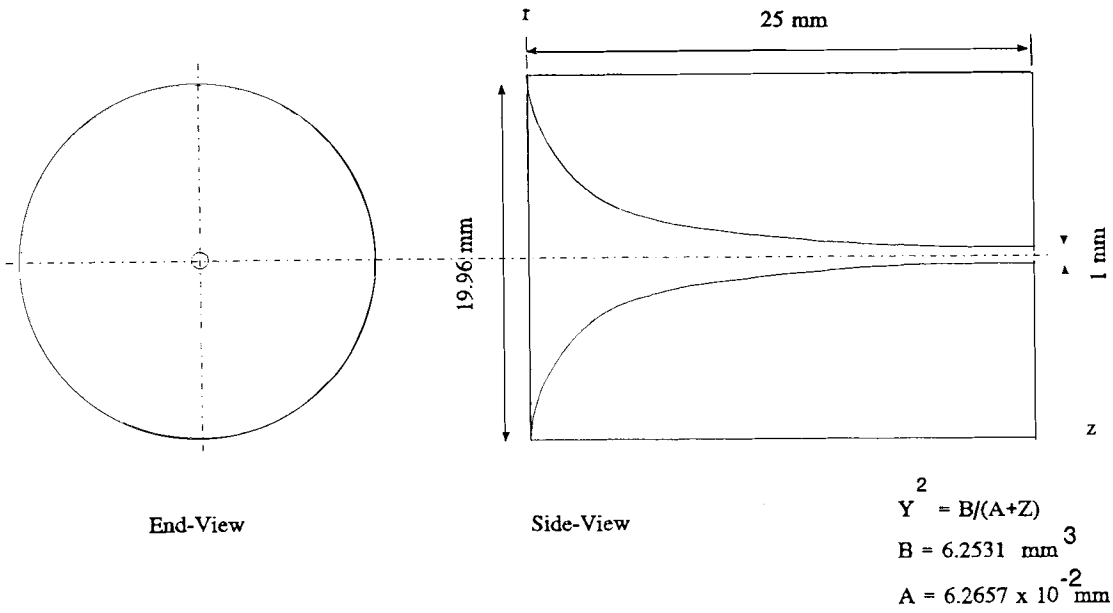

Figure 2 Hyperbolic conical die used in ACER for elongational rheometry.

tical analysis to compute the standard deviation of the raw data for the pressure drop was carried out. The pressure and the corresponding speeds were then smoothed and plotted. The elongational viscosity parameters were determined separately on a spreadsheet (Quattro Pro). In the case of shear viscosity measurements, the rheological plots were obtained using the ACER software.

Billet Preparation

Pelletized Sample

A mold for the billet was made from a copper tube of size $\frac{7}{8}$ in. BWD gauge 18 (ID 19.7 mm). The above size of the tube was chosen as it resulted in a billet that fit closely in the barrel of the ACER. A flange was welded on one end of the tube and the other end was kept free. The flange was fitted in place of the slit die on the coextrusion assembly. The tube was sprayed with a mold-release agent from inside and the extrudate was charged in from the two extruders. The gear pump rpm were adjusted to maintain the required flow rate ratio. The tube was insulated, the flanges were clamped, and the coextrusion was started. When the tube was filled with the polymer, the extrusion was stopped and the tube was detached and quenched in ice-water. The billet was then removed and cut to sample lengths (4–8 in.).

It was possible to pull the inner solid cylinder of the core polymer out of the surrounding shell since the skin and core polymer melts were immiscible. The resulting shell and core were observed for irregularities and only smooth and regular samples were accepted for runs.

Powdered Sample

A billet was first made using only the skin material following the above procedure. A hole of 13.5 mm diameter was drilled on one end of the billet using a lathe until 10 mm length of material remained at the other end, resulting in a hollow cylinder with one end closed for sealing. The powdered core material was then compacted in the shell. The shell was sealed on the open end using the skin material to prevent spilling or contamination of the core polymer.

THEORY

Assumptions

The following assumptions were made to analyze the elongational flow in the core. Since these assumptions are critical in defining the problem, each has been discussed in detail in this section:

1. The flow is incompressible. This assumption is generally valid for rheological applications[14] since compressibility effects are negligible as compared to the material effects.

Table I Geometrical Constants in the Hyperbolic Die

Geometry	Constants
Planar	$A = 4.3942$ mm $B = 43.096$ mm^2
Uniaxial	$C = 6.2531$ mm^3 $D = 6.2657 \times 10^{-2}$ mm

2. The core (the material to be analyzed) is assumed to be in pure elongational flow and the elongational strain rate is constant. This is the key assumption in this analysis. Earlier work by this research group[17] shows that imposing previously mentioned conditions in a skin–core coextrusion in a hyperbolic converging die results in a constant and essentially shear-free elongational flow.
3. The skin and core melts are completely immiscible. For the materials used in this work, experimental evidence[17] for polypropylene and polyethylene supports this assumption.
4. The flow is in a steady state. Experimental evidence for slit geometry suggests that the flow is steady in an Eulerian sense, i.e., the velocity at a fixed point in the coordinate system does not change with time. Unfortunately, due to the construction of the rheometer, it has not been possible to collect experimental evidence to prove or disprove the assumption in the case of uniaxial geometry. However, an instability for only polypropylene melts in a critical strain rate range (at about 1 s^{-1}) has been observed. This phenomena has been observed by other workers as well.[19]

The flow is, however, not steady in a Lagrangian sense, i.e., after entering the elongational flow field, a fluid element continues to deform for a finite length of time. Several workers[3] reported a dependence of the elongational viscosity of polymer melts on the applied *strain* and not the strain rate up to a Hencky strain of 3.5–4. Essentially, this phenomenon is the manifestation of the viscoelastic nature of the polymer melts.

Development

The effect of imposing the flow rate and viscosity ratio on the flow is that, whereas a significant part of the shear is pushed in the skin, the elongational flow is the dominant mode of flow in the core. The following treatment refers only to the core material, as the flow rate of the core is known and the interface (experimentally verified for the planar case) is assumed to follow the hyperbolic profile. Since according to Han[18] the pressure drop for both phases (skin and core) are the same, the treatment is further simplified.

Elongational viscosity for the planar and uniaxial geometries is defined as

$$\eta_{EP}(\dot{\epsilon}) = \frac{\tau_{xx} - \tau_{yy}}{\dot{\epsilon}} \tag{3}$$

$$\eta_{E}(\dot{\epsilon}) = \frac{\tau_{zz} - \tau_{rr}}{\dot{\epsilon}} \tag{4}$$

in terms of the stress terms and the elongational strain rates. The subscripts EP and E are used to denote the planar and uniaxial elongational viscosity, respectively. The strain rates in terms of the experimentally determined parameters (die design parameters and the process parameters) can be shown to be[15]

$$\dot{\epsilon} = \frac{Q}{2WB} \tag{5}$$

for slit geometry, and

$$\dot{\epsilon} = \frac{Q}{\pi C} \tag{6}$$

for uniaxial geometry. The values of the geometrical constants A, B, C, and D are listed in Table I.

Based on the above assumptions, the force balance as shown in Figure 3, in the flow direction (indicated by subscript 1) leads to

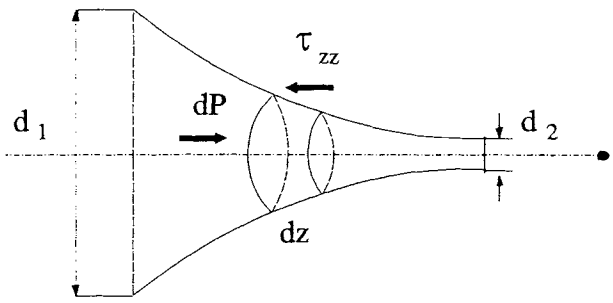

Figure 3 Force balance on the core across a converging die.

$$\tau_{11}\, dA = A\, dP \tag{7}$$

$$\Rightarrow \tau_{11} \cdot \int_{A_1}^{A_2} d\ln(A) = \int_{P_1}^{P_2} dP \tag{8}$$

Subscript 11 is used as a generic principle flow directional stress component on a surface whose normal is in the same direction, irrespective of the geometry used.

Two implicit assumptions have been made in going from eq. (7) to eq. (8). The first assumption is that the pressure P is the average pressure acting on the area normal to the flow axis. The pressure measurement was made at the die entry with a pressure transducer that was flush with the die surface. Using the momentum balance equations, it can be shown[15] that the numerical error caused by this assumption is less than 0.01% of the range of the pressure transducer. The second assumption in the above step is that τ_{11} is constant. A constant strain rate $\dot{\epsilon}$ is induced on the flow by the virtue of the die design, and by assuming that the stress state in the flow is uniquely determined by the strain rate state, it follows that τ_{11} should be constant along the flow.

For slit geometry, integrating between the limits, with the area of the slit die going from A_1 ($=2Wy_1$) to A_2 ($=2Wy_1$) and pressure going from P_1 to P_2, we get

$$\tau_{xx} = \frac{\Delta P}{\ln(y_1/y_2)} \tag{9}$$

W is the width of the slit die in the neutral axis, and y_1 and y_2 are the half-heights of the die opening at the entrance and the discharge end, respectively.

For uniaxial geometry, integrating between the limits, with the area of the circular die going from A_1 ($=\pi d_1^2/4$) to A_2 ($=\pi d_2^2/4$) and pressure going from P_1 to P_2, we get

$$\tau_{zz} = \frac{\Delta P}{2\ln(r_1/r_2)} \tag{10}$$

where d_1 and d_2 are, respectively, the entry and the exit diameters of the die.

The incompressibility assumption states[20] that

$$\nabla \cdot \nu = 0 \tag{11}$$

$$\Rightarrow d_{xx} + d_{yy} + d_{zz} = 0 \tag{12}$$

where d_{ii} is the principal component of the deformation tensor.

1. For planar geometry in the flow field defined in Cartesian coordinates, this implies that

$$\frac{\partial \nu_x}{\partial x} + \frac{\partial \nu_y}{\partial y} + \frac{\partial \nu_z}{\partial z} = 0 \tag{13}$$

$$d_{xx} = \frac{\partial \nu_x}{\partial x} = \dot{\epsilon} \tag{14}$$

$$d_{yy} = \frac{\partial \nu_y}{\partial y} = -\dot{\epsilon} \tag{15}$$

$$d_{zz} = \frac{\partial \nu_z}{\partial z} = 0 \tag{16}$$

Therefore, the transverse direction deformation rate is equal to the negative of the flow direction deformation rate and the same relationship between stress components also occurs when the assumption that the stress state is uniquely determined by the strain rate state is made. Consequently,

$$d_{yy} = -d_{xx} \tag{17}$$

$$\tau_{yy} = -\tau_{xx} \tag{18}$$

$$\tau_{xx} - \tau_{yy} = 2\tau_{xx} \tag{19}$$

The planar elongational viscosity as defined in eq. (3) can then be calculated for the core material using the equation above and the expression for the elongational strain rate [eq. (5)]:

$$\eta_{EP} = \frac{2WB}{\ln(y_1/y_2)} \frac{\Delta P}{Q} \tag{20}$$

2. For cylindrical coordinates,

$$d_{rr} + d_{\theta\theta} + d_{zz} = 0 \tag{21}$$

$$d_{rr} = \frac{\partial \nu_r}{\partial r} = -\frac{\dot{\epsilon}}{2} \tag{22}$$

$$d_{\theta\theta} = \left(\frac{1}{r}\frac{\partial \nu_\theta}{\partial \theta} + \frac{\nu_r}{r}\right) = \frac{\nu_r}{r} = -\frac{\dot{\epsilon}}{2} \tag{23}$$

$$d_{zz} = \left(\frac{\partial \nu_z}{\partial z}\right) = \dot{\epsilon} \tag{24}$$

Therefore, the transverse direction deformation rate is equal to hoop direction deformation rate, and they are both equal to the negative of half the flow direction deformation rate. The same relationship between

Table II Shear Viscosity of Polyethylene Melts

Strain Rate ($\dot{\gamma}$)	PE (Pa-s) DOW 2503 (290°C)	DOW LDPE
13.48	—	89.12
26.91	48.97	79.43
53.70	30.90	77.62
107.15	22.38	69.18
269.15	17.37	67.61
537.03	13.18	58.88
1318.3	—	46.77
2691.5	—	38.01

stress components also occurs if the assumption similar to the one made in the planar case—that the stress state is uniquely determined by the strain rate state—is made. Therefore,

$$d_{\theta\theta} = d_{rr} = -\frac{\dot{\epsilon}}{2} = -\frac{1}{2} d_{zz} \tag{25}$$

$$\Rightarrow \tau_{\theta\theta} = \tau_{rr} = -\frac{1}{2} \tau_{zz} \tag{26}$$

The uniaxial elongational viscosity as defined in eq. (4) can be calculated for the core from the equation above and from the elongational strain rates [eq. (6):

$$\eta_E = \frac{3\pi}{4} \frac{C}{\ln(r_1/r_2)} \frac{\Delta P}{Q} \tag{27}$$

In both cases, the elongational viscosity is obtained as a product of two terms: one term containing the geometric or the die design parameters and the other term containing the process parameters to be measured in the experiment, namely, the pressure drop across the die and the flow rate of the core.

MATERIALS

The following core materials were used for the elongational rheology: commercial grade polypropylenes, syndiotactic polystyrene, and nylon-66. Commercial grades of polyethylene were used as the skin material all the grades of core polymers.

Polyethylene

The following grades of polyethylene were used in the work: DOW 2503 and DOW LDPE. In addition, the grade DOW LLD-2 was used in the tracer particle measurement in the planar die. The zero shear viscosity of this grade was 63 Pa-s at 200°C. Table II lists the shear viscosities of the above grades measured in the ACER.

Polypropylene

The polypropylene grades were provided by Phillips 66. HGX 030 and HGZ 200 were used in the experiments. The details of the material supplied by Rheometrics Inc. were not available from the supplier. Table III lists the shear viscosities of the above grades measured in the ACER. In addition, grade HGY 040 was used in the planar rheometer to perform the tracer particle measurement. The zero shear viscosity of the sample was 77,382 Pa-s at 200°C. The molecular weight of HGX 030 was 300,000 and the polydispersity index (M_w/M_n) was between 4 and 6.[19]

Nylon-66

Nylon-66 was supplied by DuPont. The melting point of the sample was 280°C and the material was available in a powdered form. The operating temperature was 290°C. Prior to the analysis, the sample was dried for 4 h at 60°C under nitrogen to remove moisture. This procedure is essential to prevent degradation of nylon at elevated temperature. The polydispersity index of this sample was reported to be 2.[21]

Table III Shear Viscosity of Polypropylene Melts at 200°C

Strain Rate ($\dot{\gamma}$)	PP (Pa-s) HGX 030	HGZ200
13.48	3235.9	1513.5
26.91	2344.2	831.76
53.70	1479.1	645.65
107.15	933.32	512.86
269.15	501.12	288.40
537.03	309.12	177.82
1318.3	158.50	93.32
2691.5	95.49	60.25

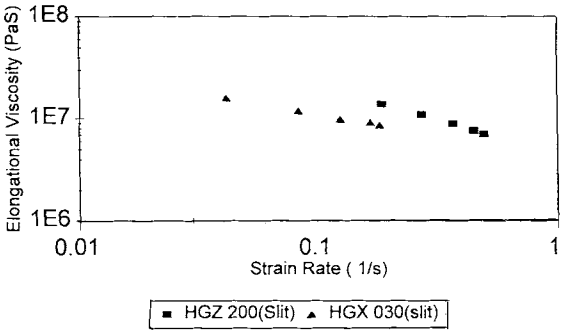

Figure 4 Planar elongational viscosity of HGX 030 and HGZ 200 at 200°C as a function of elongational strain rate.

Syndiotactic Polystyrene

Syndiotactic polystyrene was supplied by Dow Chemicals. The melting point of the material was 280°C. The analysis of the material was carried out at two operating temperatures, 290 and 300°C. The molecular weight of the sample was 4.5×10^5 with the polydispersity index of 2.5.

RESULTS AND DISCUSSION

Planar Elongational Viscosity

Two commercial grades of polypropylene (HGX 030 and HGZ 200) were used for planar elongational viscosity determination in the slit rheometer. Figure 4 shows the planar elongational viscosity of the two polymer melts measured at 200°C. The pressure drop data obtained were very stable; the standard deviation obtained for the data was smaller than the size of the data points.

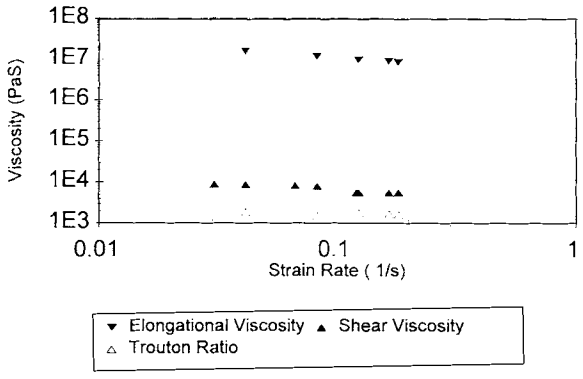

Figure 5 Shear viscosity and planar Trouton ratio of HGX 030 at 200°C at shear rates equivalent to applied elongational strain rates.

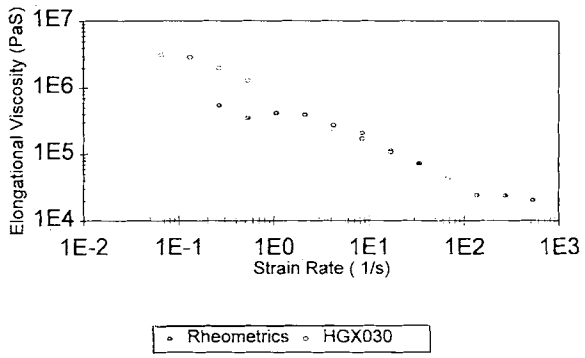

Figure 6 Uniaxial elongational viscosity of polypropylenes at 200°C as a function of elongational strain rate.

The planar elongational viscosity of polypropylene melts in the given extensional rate range decreases with increasing strain rate. Recent work on polypropylene melts at lower or comparable strain rates[22] indicated that, except at very small strain rates (10^{-3} s^{-1}), polypropylene melts show a strain thinning behavior as indicated in this work. The above trend has been also observed at higher strain rates in uniaxial geometry. As reported by several workers,[13,14] the observed Trouton ratio (Fig. 5) is higher by 2–3 orders of magnitude than the theoretically predicted value of 4 for Newtonian fluids.

Uniaxial Elongational Viscosity

Two commercial grades of polypropylene, syndiotactic polystyrene and nylon-66 melts, were analyzed in the uniaxial geometry rheometer. The uniaxial elongational viscosity of HGX 030 and the Rheometrics sample at 200°C as a function of the elongational strain rate is presented in Figure 6. The Trouton ratio as a function of the strain rate at 200°C is presented in Figure 7.

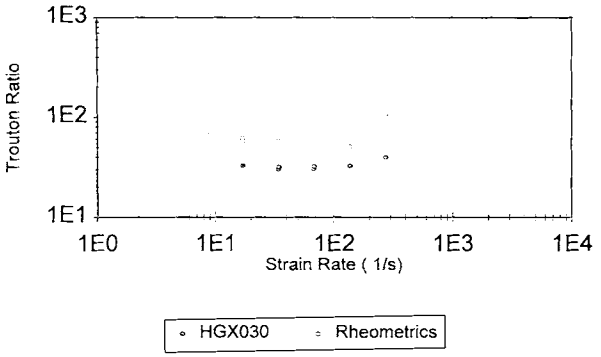

Figure 7 Trouton ratio of polypropylenes at 200°C at shear rates equivalent to applied elongational strain rates.

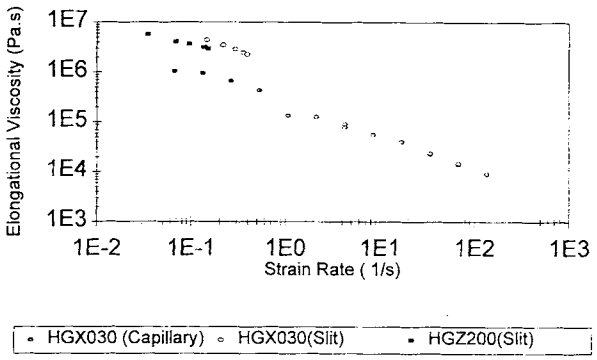

Figure 8 Normalized planar and uniaxial viscosity of HGX 030 at 200°C.

As observed for the planar case, a strain thinning behavior in the sample is also observed in uniaxial geometry. At equivalent strain rates ($< 50\ s^{-1}$), the data agree within an order of magnitude with that presented in the literature.[22] At higher strain rates ($> 100\ s^{-1}$), data were not available in the literature to compare.

An anomaly in the data appeared at the strain rate of $1\ s^{-1}$. The anomaly is in the form of an instability in the pressure drop which resulted in a deviation from the trend. Several researchers in industry[19,23] have reported a similar instability in the shear mode occurring at the corresponding stress level (0.1–1 MPa). In the literature, the phenomenon has been reported but is not well understood.[14]

The Trouton ratio of HGX 030 in the uniaxial geometry (Fig. 7) is higher than the theoretical limit of 3. The ratio reaches a near constant value at strain rates higher than $50\ s^{-1}$. To compare the two geometries, the elongational viscosity data for the planar and the uniaxial case were normalized. The planar viscosity data were divided by the theoretical value (for Newtonian flow) of 4 and the uniaxial data were divided by the equivalent value of 3. Thus, for the same strain rate range, if the molecular motions were the same, the two sets of data would be expected to coincide. The resulting data are plotted on Figure 8. Qualitatively, the trends agree but the normalized planar elongational viscosity is higher than the normalized uniaxial elongational viscosity. The possible source of mismatch could be the fact that the Hencky strain in the planar case was 3.08, and the flow could still be in the transient phase. Other possible source could be in the difference in the geometry of the feeding section and the die flow channel and the placement of the pressure transducer. A circular pipe feeds the melt into the rectangular slit geometry, and this change in the flow profile could be affecting the data. It should be noted that these effects are minimized in the conical geometry by designing the entry diameter of the hyperbolic conical die to be the same as the diameter of the feeding barrel. It could also be argued that since the planar and uniaxial viscosities are essentially the manifestation of the motion of molecules in different geometries, the quantitative results may be different in each case.

Syndiotactic Polystyrene (sPS)

The material was analyzed at two operating temperatures: 280 and 300°C. Since the material was prone to thermal degradation at elevated temperature, the thermal history of this sample differed from the rest of the materials. The material was first heated to 200°C (where it was stable) for 15 min and then heated to the operating temperature and maintained there for 15 min prior to starting the experiment.

The elongational viscosity of the sample at the two operating temperatures is plotted in Figure 9. The Trouton ratio and the shear viscosity of the sample at 300°C are also shown. Stable results for strain rates higher than $10\ s^{-1}$ were not obtained for the sPS melt. In the observed range, the elongational viscosity of sPS samples decreases with the strain rate. The decrease is sharper than that observed for polypropylene melts. No data on the elongational viscosity of sPS were available for comparison. As expected, the elongational viscosity of sPS decreased with an increase in the temperature. The strain thinning was steeper at 300°C than that at 280°C. The Trouton ratios were smaller than those observed for polypropylene melts. The Trouton ratio seems to decrease slightly with increasing strain rate in the observed range.

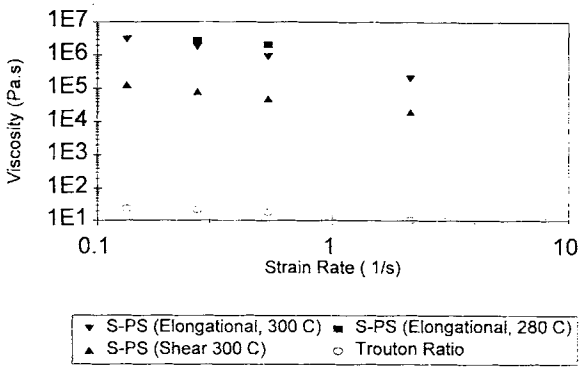

Figure 9 Elongational viscosity, shear viscosity, and Trouton ratio of syndiotactic polystyrene melt at 280 and 300°C.

Nylon-66

The operating temperature for this sample was 290°C. Figure 10 presents the elongational viscosity data obtained for the sample. The Trouton ratio and the shear viscosity are also plotted in the figure. An apparent slight initial increase in the elongational viscosity with increasing strain rate is observed followed by an apparent peak at strain rate of 2–5 s^{-1}. The increase is significantly higher than the standard deviation of the data. At higher strain rates, the viscosity drops, showing strain thinning behavior. In the available literature, there was no elongational rheology data on this material at the strain rates generated in this work. However, the slight increase and then the drop at 1 s^{-1} is consistent with observed behavior in industry for spinning nylon-66.[21] This is a deviation from the shear rheology of the material where the shear viscosity remains nearly constant at shear rates 1–10 s^{-1} and then slightly drops with increasing shear rate for shear rates greater than 100 s^{-1}.

The Trouton ratio of the sample was two orders of magnitude higher than the theoretical limit of 3 for a Newtonian fluid. The Trouton ratio as a function of strain rate nearly follows the elongational viscosity curve, primarily because at the induced strain rate range the shear viscosity is found to be nearly constant.

Effect of Molecular Parameters

Figure 11 shows a plot of the Trouton ratios of HGX 030, nylon-66, and syndiotactic polystyrene. The polydispersity index of each melt is indicated in the legend. The data indicate that the spread of the molecular weight may affect the dependence of the Trouton ratio on the elongational strain rates. The Trouton ratio decreases with increasing strain rate

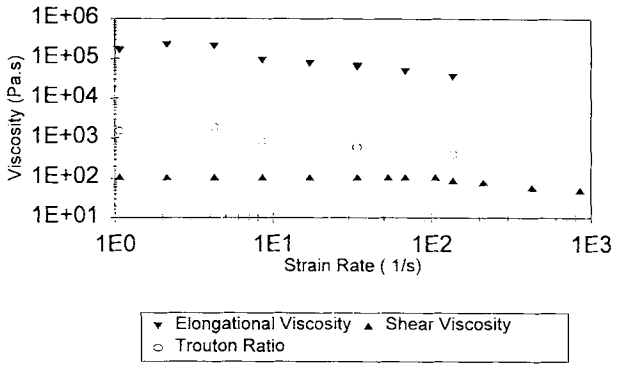

Figure 10 Elongational viscosity, shear viscosity, and Trouton ratio of nylon-66 melt 290°C.

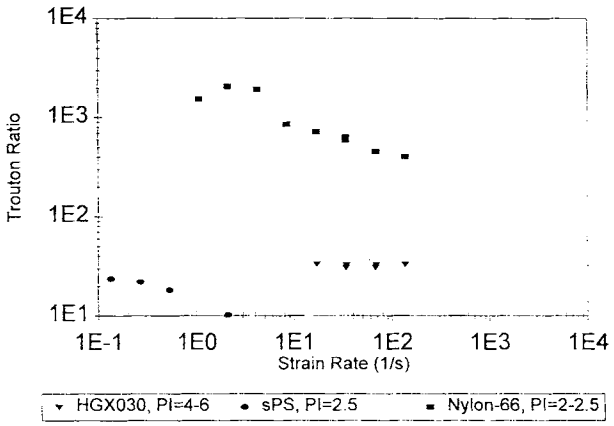

Figure 11 Correlation between the Trouton ratio and polydispersity index of polymer melts.

for a narrow distribution (PI = 2–2.5) of molecular weight, for nylon-66 and syndiotactic polystyrene melts in this case. For a broader molecular spread polymer (PI = 4–6), e.g., polypropylene, the Trouton ratio seems to be relatively insensitive to the strain rate. A sharper shear thinning behavior of narrow molecular weight distribution polymers as compared to a more diffused shear thinning behavior of broad molecular weight distribution polymers is well known in shear viscosity,[7,14] but a similar study in elongational behavior is not available. A recent study on the effect of branching on polyethylene[24] concluded that the elongational viscosity is dependent on the degree of branching present in the molecule structure. The present data indicate a correlation between the elongational rheology and the molecular weight distribution of the polymer melt. More detailed study is desirable in this area.

CONCLUSIONS

It is possible to generate nearly shear-free elongational flow in a core polymer melt using the skin–core coextrusion process by imposing conditions on the skin-to-core viscosity ratio and flow rate ratio. The conditions necessary to develop pure elongational flow in the core are that the flow rate ratio of core to skin should be about 10 and the viscosity ratio should be at least 10^2. A laboratory-scale planar rheometer to study the elongational rheology of polymer melts was developed by coupling the above two concepts. Implementation of the process on a commercial capillary rheometer (ACER) was carried out by replacing the standard capillary die by a conical hyperbolic converging die. A patent has been issued on the process.[25]

Stable flows are observed in the planar elongational rheometer. The stability of flow in the uniaxial geometry was not able to be confirmed experimentally due to the inability of visual observation of the melt. Stability parameters calculated for the entry flow to the uniaxial elongational rheometer indicate a stable flow prior to the die entry. It was experimentally observed that in a critical range of strain rates (0.5–3 s^{-1}) the coextruded flow can become unstable; however, the flow was found to be stable above and below the critical limits. The range of the observed instability agrees with the literature and industrial observations. The instability could be due to interfacial slippage; however, more work is needed in this area to correlate the theoretical analysis with the observed behavior.

It was possible to generate strain rates up to 533 s^{-1} in the uniaxial rheometer. Commercial grades of polypropylene, syndiotactic polystyrene, and nylon-66 melts were analyzed. Polyethylene was used as a skin layer in all the experiments. General agreement with the available literature for equivalent strain rates was found. It can be concluded from the data obtained that the elongational rheometer developed in this work can detect a significant rheological response of polymer melts to induced stress that cannot be characterized by shear rheology alone. The design of the rheometer does not allow measurement of the transient behavior of polymer melts. Analysis of the core polymer melt requires a choice of appropriate lubricant or skin to be made.

Financial support from Polymer Laboratories, U.K. (now Rheometrics Inc., U.S.A.), and NSF (Grant Numbers DMC 8896Q30 and DMR 9202434) is gratefully acknowledged. The authors would also like to thank Dr. Frank Baker of Rheometrics Inc. and Dr. Roger Ross and Dr. Steven Threefoot of DuPont for their valuable suggestions during the research.

REFERENCES

1. K. Walters, *Rheometry: Industrial Applications,* Research Studies Press, Wiley, New York, 1980.
2. J. M. Dealy and K. F. Wissbrun, *Melt Rheology and Its Role in Plastics Processing, Theory and Applications,* Van Nostrand Reinhold, New York, 1990.
3. J. Ferguson and Z. Kemblowski, *Applied Fluid Rheology,* Elsevier, New York, 1991.
4. H. A. Barnes, J. F. Hutton, and K. Walters, *An Introduction to Rheology,* Rheology Series, 3, Elsevier, Amsterdam, 1989.
5. R. K. Prud'homme and G. G. Warr, *Langmuir,* **10**(10), 3419–3426 (1994).
6. K. W. Jansson, L. Bohlin, and A. Eliasson, *Rheology,* **4,** 192–197 (1994).
7. F. N. Cogswell, *Polymer Melt Rheology; A Guide for Industrial Practice,* Wiley, New York, 1981.
8. J. Meissner, *Trans. Soc. Rheol.,* **16,** 405–420 (1972).
9. C. J. S. Petrie, *Elongational Flows,* Research Notes in Mathematics, Pittman, London, UK, 1979.
10. M. T. Shaw, *J. Appl. Polym. Sci.,* **19,** 2811–2816 (1975).
11. A. E. Everage and R. L. Ballman, *Nature,* **273,** 213–215 (1978).
12. H. H. Winter, C. W. Macosko, and K. E. Bennet, *Rheol. Acta,* **18,** 323 (1979).
13. M. E. Mackay and A. M. Dajan, *J. Rheol.,* **39**(1), 1–14 (1994).
14. C. W. Macosko, *Rheology: Principles, Measurements, and Applications,* VCH, New York, 1994.
15. A. V. Pendse, PhD Dissertation, Louisiana State University, 1995.
16. D. F. James, in *Recent Developments in Structured Continua,* D. DeKee and P. N. Kaloni, Eds., Longman, London, 1990.
17. H. C. Kim, A. V. Pendse, and J. R. Collier, *J. Rheol.,* **38,** 831–845 (1994).
18. C. D. Han, *Multiphase Flow in Polymer Processing,* Academic Press, New York, 1981.
19. J. Janzen, Personal communications, Phillips Petroleum, 1994.
20. R. B. Bird, R. C. Armstrong, and O. Hassagar, *Dynamics of Polymeric Fluids,* 2nd ed., Wiley-Interscience, New York, 1987, Vol. I.
21. R. A. Ross, Personal communications, DuPont Co., 1995.
22. R. Hingman and B. L. Marczinke, *J. Rheol.,* **38**(3), 573–587 (1994).
23. F. Baker, Personal communications, Rheometrics Inc., 1993.
24. R. K. Chohan, *J. Appl. Polym. Sci.,* **54,** 487–495 (1994).
25. J. R. Collier, U.S. Pat. 5,357,784 (1994).

Received June 2, 1995
Accepted August 28, 1995